Zeitschrift: Helvetica Physica Acta
Band: 53 (1980)
Heft: 1

Artikel: Decay electron spectra of bound muons
Autor: Herzog, F. / Alder, K.
DOI: https://doi.org/10.5169/seals-115109

Nutzungsbedingungen
Die ETH-Bibliothek ist die Anbieterin der digitalisierten Zeitschriften auf E-Periodica. Sie besitzt keine Urheberrechte an den Zeitschriften und ist nicht verantwortlich für deren Inhalte. Die Rechte liegen in der Regel bei den Herausgebern beziehungsweise den externen Rechteinhabern. Das Veröffentlichen von Bildern in Print- und Online-Publikationen sowie auf Social Media-Kanälen oder Webseiten ist nur mit vorheriger Genehmigung der Rechteinhaber erlaubt. Mehr erfahren

Conditions d'utilisation
L'ETH Library est le fournisseur des revues numérisées. Elle ne détient aucun droit d'auteur sur les revues et n'est pas responsable de leur contenu. En règle générale, les droits sont détenus par les éditeurs ou les détenteurs de droits externes. La reproduction d'images dans des publications imprimées ou en ligne ainsi que sur des canaux de médias sociaux ou des sites web n'est autorisée qu'avec l'accord préalable des détenteurs des droits. En savoir plus

Terms of use
The ETH Library is the provider of the digitised journals. It does not own any copyrights to the journals and is not responsible for their content. The rights usually lie with the publishers or the external rights holders. Publishing images in print and online publications, as well as on social media channels or websites, is only permitted with the prior consent of the rights holders. Find out more

Download PDF: 07.01.2026

ETH-Bibliothek Zürich, E-Periodica, https://www.e-periodica.ch

Decay electron spectra of bound muons

by **F. Herzog** and **K. Alder**

Institut für Physik, Universität Basel, CH-4956 Basel, Switzerland

(20. II. 1980)

Abstract. The decay electron spectrum for a bound muon in the $1s_{1/2}$ state is calculated for several elements and for the $(V-A)$, S, P and T weak interactions. Dirac wave functions have been used for the muon and the electron. The finite nuclear size and the nuclear recoil as well as the vacuum polarization are included in our computations. The influence of the bremsstrahlung emitted by the final electron on the electron energy spectrum is discussed.

I. Introduction

In the framework of modern gauge models for the electroweak interaction attempts have been made to estimate the strength of possible muon number violating processes [1]. In connection with the lepton quark generation problem the question of lepton number conservation is crucial. Thus, experiments looking for lepton processes which are strictly forbidden in the widely accepted scheme of lepton number conservation (additive lepton number conservation) have been proposed recently again. One possible test, where the additive muon number law is violated, is the study of the muon electron conversion. Experiments to investigate this type of process have been performed several times. The best known upper limit for the branching ratio of the muon number violating process relative to the ordinary muon capture was measured by the Bern group at SIN and found to be for sulphur [2]:

$$\sigma(\mu^- {}^{32}\mathrm{S} \rightarrow e^- {}^{32}\mathrm{S})/\sigma(\mu^- {}^{32}\mathrm{S} \rightarrow \text{capture}) < 7 \times 10^{-11} (90\% \text{ C.L.})$$

In order to interpret a possible signal for muon electron conversion correctly one has to know the backgrounds very accurately. Besides radiative muon capture followed by internal or external γ-conversion, bound muon decay is the most important background entering into muon electron conversion experiments.

The decay process of a negative muon bound in the ground state of an atom is known to be modified relative to the free muon decay. The first difference arises from the momentum distribution of the bound muon and results in a reduction of the phase space accessible to the particles in the final state as well as in Doppler broadening of the bound muon deday electron spectrum (BOMES). This phase space effect diminishes the decay rate of bound muons relative to that of free muons. A second reduction takes place because of the time dilatation of the muon lifetime in the restframe of the muonic atom. The Coulomb force acting on the outgoing electron is responsible for the third difference; this final state interaction leads to an increase of the bound muon decay relative to the free decay rate,

because of the greater overlap of the muonic and electronic wave functions in the case of bound muon decay. For a more qualitative treatment of bound muon decay physics the reader is referred to Refs. [3], [4], [5] and [6].

From an experimental point of view it is still impossible to exclude satisfactorialy few precent admixtures of scalar (S), pseudoscalar (P) and tensor (T) couplings to the well-known $V-A$ weak interaction [7]. Therefore, we have calculated the BOMES also with these couplings, in the hope that future experiments on this subject will give more exact information.

In section II we derive expressions for the BOMES assuming $(V-A)$, $S(P)$ and T Fermi couplings. Numerical results of the BOMES for several elements which have been and are in discussion for muon electron conversion experiments ([8], [9], [10]) are listed in Section III. Section IV is devoted to an estimate of the bremsstrahlung effect of the emitted electron on the shape of BOMES. The discussion of our results is the content of the last section.

The notation as well as the electron- and muon-wavefunctions used in our calculations are presented in appendices.

II. Exact expressions for the electron spectrum resulting from muon decay in the ground state of an atom with charge number Z.

We are looking at the process shown in Fig. 1. The bubble therein means an effective electromagnetic as well as weak coupling. Since the ratio of the muon to W-boson mass is thought to be very small, we take as weak effective coupling the Fermi four fermion interaction. The contributions to the effective electromagnetic coupling are given graphically in Fig. 2.

In order to derive BOMES expressions for the $(V-A)$, S, P and T interaction, the general starting point is the weak charge retention ordered Lagrangian L^F ([7], [11] and appendix A).

$$L_i^F = \frac{g_i}{\sqrt{2}} \psi_e^+(x)\gamma_0 O_i \psi_\mu(x) \psi_{\nu_\mu}^+(x)\gamma_0 O^i \psi_{\bar{\nu}_e}(x) + \text{hermitian conjugate} \qquad (1).$$

The g_i are the coupling constants where the index i refers to the four different

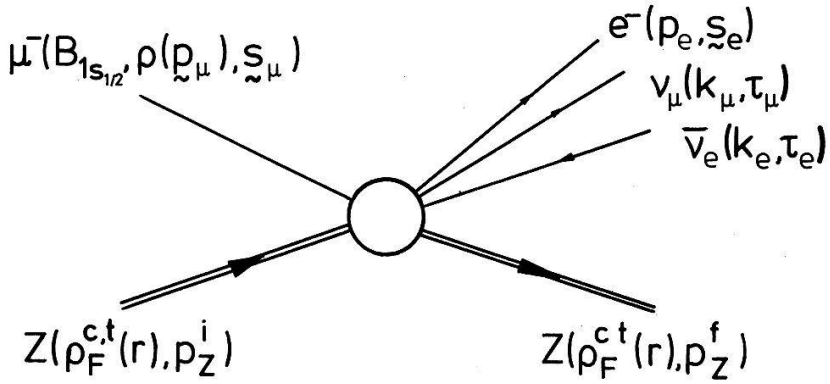

Figure 1
Diagram of the weak decay of a $1s_{1/2}$ muon. The muon μ is characterized by its momentum distribution $\rho(\mathbf{p}_\mu)$, its energy eigenvalue in the ground state $-B_{1s_{1/2}}$ and its polarization $\mathbf{s}_\mu$. The other leptons are all characterized by their four-momentum (p_e for e^-, k_μ for ν_μ and k_e for $\bar{\nu}_e$) and their polarization ($\mathbf{s}_e$ for e^-, τ_μ for ν_μ and τ_e for $\bar{\nu}_e$). We treat the nucleus with charge number Z as spinless particle, parametrized by a Fermi charge distribution $\rho_F^{c,t}(r)$ (c, t = Fermi parameters), with initial four-momentum p_Z^i and final four-momentum p_Z^f.

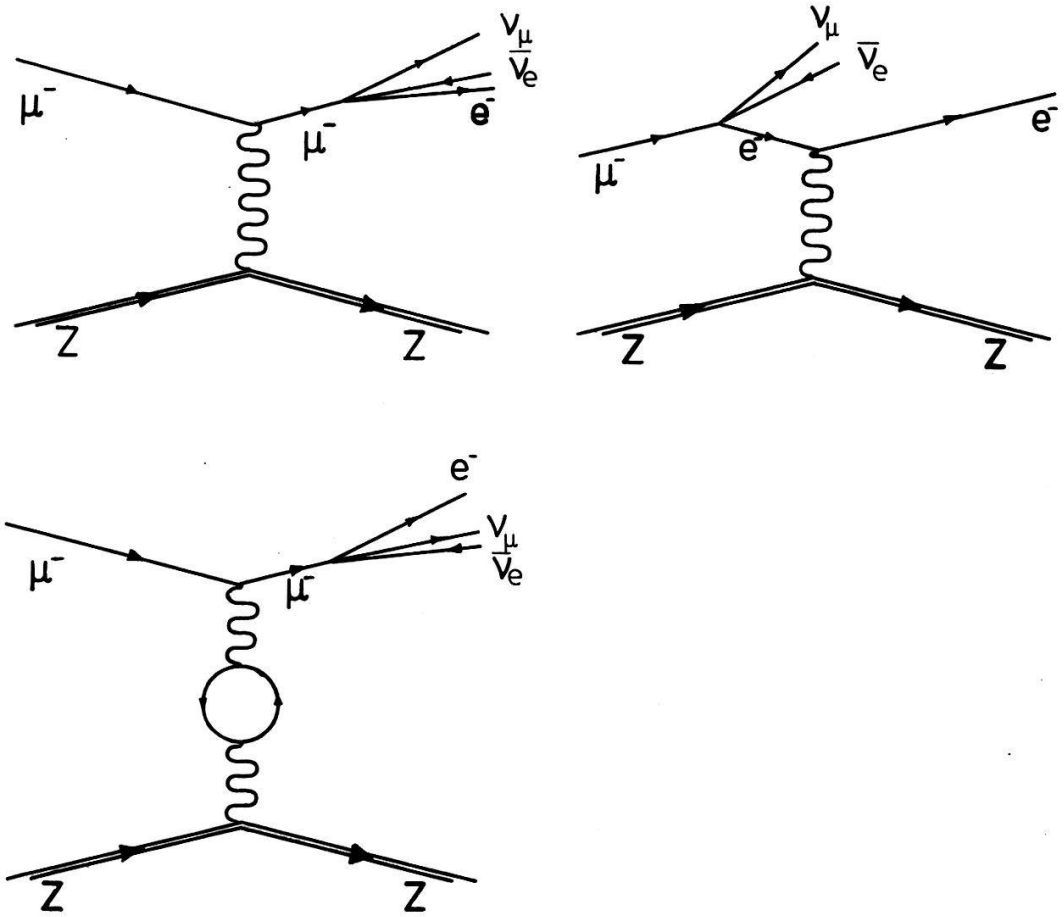

Figure 2
Contributions to the effective electro-magnetic coupling, which are incorporated in our calculations.

interaction types $(V-A)$, S, P and T.[1]) The O_i are the corresponding interaction operators, given as combinations of Dirac matrices. The $\psi_\alpha(x)$ is the field operator of particle α at the point x of the spacetime continuum.

We are interested in the matrix elements $\langle e^-, \bar{\nu}_e, \nu_\mu \,|T^i_{\text{lep}}|\, \mu\rangle$ of the pure leptonic decay operator T^i_{lep} which can be derived from equation (1):

$$\langle e^-, \bar{\nu}_e, \nu_\mu \,|T^i_{\text{lep}}|\, \mu\rangle = \frac{g_i}{\sqrt{2}} \int d^4x \varphi_e^+(p_e, \mathbf{s}_e, x)\gamma_0 O_i \varphi_\mu(B_{1s_{1/2}}, \rho(\mathbf{p}_\mu), \mathbf{s}_\mu, x)\varphi^+_{\nu_\mu}(k_\mu, \tau_\mu, x)\gamma_0 O^i \varphi_{\bar{\nu}_e}(k_e, \tau_e, x) \quad (2)$$

Here $\varphi_\mu(B_{1s_{1/2}}, \rho(\mathbf{p}_\mu), \mathbf{s}_\mu, x)$ is the wave function of the groundstate muon characterized by the energy eigenvalue $-B_{1s_{1/2}}$ the momentum distribution $\rho(\mathbf{p}_\mu)$ and the polarization $\mathbf{s}_\mu$. $\varphi_e(p_e, \mathbf{s}_e, x)$ is the electron wave function with asymptotic four-momentum p_e and polarization $\mathbf{s}_e$. According to Fig. 2 the neutrino wave functions $\varphi_{\nu_\mu}(k_\mu, \tau_\mu, x)$ and $\varphi_{\bar{\nu}_e}(k_e, \tau_e, x)$ are Dirac plane waves. For plane waves we choose the standard momentum normalization as in Ref. [12]. With the

[1]) (Since we are only interested in the electron energy spectra, there are no mixing terms between parity conserving and parity non-conserving couplings; therefore parity violation is of no importance in this connection).

notation $x=(t,\mathbf{r})$ equation (2) results in

$$\langle e^-, \bar{\nu}_e, \nu_\mu \,|T^i_{\text{lep}}|\, \mu\rangle = \frac{g_i}{\sqrt{2}}\frac{1}{(2\pi)^2}\left(\frac{m_{\bar{\nu}_e} m_{\nu_\mu}}{E_{\bar{\nu}_e} E_{\nu_\mu}}\right)^{1/2}$$
$$\times u^+_{\nu_\mu}(k_\mu, \tau_\mu)\gamma_0 O^i v_{\bar{\nu}_e}(k_e, \tau_e)\ \delta(E_\mu - E_e - E_{\bar{\nu}_e} - E_{\nu_\mu})$$
$$\times \int d^3r \varphi^+_e(p_e, \mathbf{s}_e, \mathbf{r})\gamma_0 O_i \varphi_\mu(B_{1s_{1/2}}, \rho(\mathbf{p}_\mu), \mathbf{s}_\mu, \mathbf{r}) e^{-i(\mathbf{k}_e+\mathbf{k}_\mu)\mathbf{r}} \quad (3)$$

From equation (3) one deduces the transition probability per unit time $d^{(3)}W/dt$ from the initial muon state to final states (the index 3 in $d^{(3)}W/dt$ indicates, that in principle all three final state particles are detectable):

$$\frac{d^{(3)}W_i}{dt} = \frac{g_i^2}{4}\frac{1}{(2\pi)^8}\frac{m_{\bar{\nu}_e} m_{\nu_\mu}}{E_{\bar{\nu}_e} E_{\nu_\mu}}\frac{1}{E_e}\, d^3k_e\, d^3k_\mu\, d^3p_e\, \delta(E_\mu - E_e - E_{\bar{\nu}_e} - E_{\nu_\mu})$$
$$\times \Big| u^+_{\nu_\mu}(k_\mu, \tau_\mu)\gamma_0 O^i v_{\bar{\nu}_e}(k_e, \tau_e)$$
$$\times \int d^3r \varphi^+_e(p_e, \mathbf{s}_e, \mathbf{r})\gamma_0 O_i \varphi_\mu(B_{1s_{1/2}}, \rho(\mathbf{p}_\mu), \mathbf{s}_\mu, \mathbf{r}) e^{-i(\mathbf{k}_e+\mathbf{k}_\mu)\mathbf{r}}\Big|^2 \quad (4)$$

where E_α, $\alpha = e^-, \nu_\mu, \bar{\nu}_e$ is the total energy of particle α and E_μ the total energy of the bound muon, $E_\mu = \bar{m}_\mu - B_{1s_{1/2}}$ ($\bar{m}_\mu$ = reduced muon mass $\approx m_\mu$. We use the fact that the nucleus has a nearly nonrelativistic motion).

Since no neutrinos are dedected in nowadays muon decay experiments, we sum over τ_μ, τ_e and integrate over the two momenta $\mathbf{k}_\mu$, $\mathbf{k}_e$ (thereby we take both neutrinos as massless particles):

$$\frac{d^{(1)}W_i}{dt} = \sum_{\tau_e,\tau_\mu}\int d^3k_e \int d^3k_\mu \frac{d^{(3)}W_i}{dt} = \frac{g_i^2}{2^4(2\pi)^8}\frac{d^3p_e}{E_e}$$
$$\times \int \frac{d^3k_e}{E_{\bar{\nu}_e}}\int \frac{d^3k_\mu}{E_{\nu_\mu}} \operatorname{tr}\{(O_i)_{\lambda\mu\ldots}\not{k}_e (O_i)_{\sigma\tau\ldots}\not{k}_\mu\}\ \delta(E_\mu - E_e - E_{\bar{\nu}_e} - E_{\nu_\mu})$$
$$\times J^{\lambda\mu\ldots}_{O_i}(p_e, \mathbf{s}_e, B_{1s_{1/2}}, \rho(\mathbf{p}_\mu), \mathbf{s}_\mu, \mathbf{P}) J^{\sigma\tau *}_{O_i}(p_e, \mathbf{s}_e, B_{1s_{1/2}}, \rho(\mathbf{p}_\mu), \mathbf{s}_\mu, \mathbf{P}) \quad (5)$$

We have used the following notation

$$\mathbf{P} = \mathbf{k}_e + \mathbf{k}_\mu$$

$$J^{\lambda\mu\ldots}_{O_i}(p_e, \mathbf{s}_e, B_{1s_{1/2}}, \rho(\mathbf{p}_\mu), \mathbf{s}_\mu, \mathbf{P}) = \int_0^\infty d^3r \varphi^+_e(p_e, \mathbf{s}_e, \mathbf{r})\gamma_0 O^{\lambda\mu\ldots}_i \varphi_\mu(B_{1s_{1/2}}, \rho(\mathbf{p}_\mu), \mathbf{s}_\mu, \mathbf{r}) e^{-i\mathbf{P}\mathbf{r}}$$

$$(O_i)_{\lambda\mu\ldots} = \begin{cases} 1 & S \text{ interaction operator} \\ \gamma_5 & P \text{ interaction operator} \\ \gamma_\lambda(1-\gamma_5) & V-A \text{ interaction operator with } \gamma_5 = i\gamma_0\gamma_1\gamma_2\gamma_3 \\ \sigma_{\lambda\mu} & T \text{ interaction operator} \end{cases}$$

To proceed in the evaluation of $d^{(1)}W/dt$ given by equation (5) we have to treat the calculation for the different coupling types separately.

II.1. *Bound nuon electron spectrum assuming* $(V-A)-$*interaction*

In this physically most important case the trace in equation (5) is simple. We evaluate the integrations over $\mathbf{k}_e$ and $\mathbf{k}_\mu$ and find

$$\frac{d^{(1)}W_{V-A}}{dt}=\frac{g_{VA}^2}{6(2\pi)^7}\frac{d^3p_e}{E_e}\int d\Omega(\hat{\mathbf{P}})\int^{P^{\max}} d\,|\mathbf{P}|\,|\mathbf{P}|^2\{P_\lambda P_\rho-g_{\lambda\rho}P^2\}$$
$$\times J_{VA}^{\lambda}(p_e,\mathbf{s}_e,B_{1s_{1/2}},\rho(\mathbf{p}_\mu),\mathbf{s}_\mu,\mathbf{P})J_{VA}^{\rho *}(p_e,\mathbf{s}_e,B_{1s_{1/2}},\rho(\mathbf{p}_\mu),\mathbf{s}_\mu,\mathbf{P}) \qquad (6)$$

where $\mathbf{P}=|\mathbf{P}|\,\hat{\mathbf{P}}$.

The upper limit of the $|\mathbf{P}|$-integration is given by $P^{\max}=E_\mu-E_e=P_0$. We insert now the exact muon – and electron wave functions (appendix B) and choose a coordinate system with $\hat{\mathbf{P}}$ in z-direction, so that the integration over $\Omega(\hat{\mathbf{P}})$ can be done. Since we are not interested in the direction of $\mathbf{p}_e$ we also perform the $\Omega(\hat{\mathbf{p}}_e)$ integration. Both integrations can be done analytically. We average over the initial polarization s_μ and sum over the electron polarization states; we get for the BOMES:

$$\frac{d\Gamma^{V-A}(\mu^-+Z\to e^-+Z+\bar{\nu}_e+\nu_\mu)}{dE_e}$$
$$=\frac{g_{VA}^2 m_\mu}{3(2\pi)^3}\sum_{\kappa_e,\mu_e,s_\mu}(-1)^{2\mu_e-1}\int_0^{P^{\max}} dPP^2$$
$$\times\{(P_0^2-P^2)\,|\mathbf{J}|^2+P^2\,|J_0|^2+|\mathbf{PJ}|^2-P_0\mathbf{P}\,\mathrm{Re}\,(J_0\mathbf{J}^*)\} \qquad (7)$$

where $P=|\mathbf{P}|$ and

$$J_0=\sqrt{4\pi}\sum_{\lambda=0}^{\infty}(-i)^\lambda\sqrt{2\lambda+1}\int drr^2 j_\lambda(Pr)$$
$$\times\{(g_{\kappa_e}g_1+f_{\kappa_e}f_1)\langle\kappa_e\mu_e\,|Y_{\lambda 0}|-1s_\mu\rangle-i(g_{k_e}f_1-f_{\kappa_e}g_1)\langle\kappa_e\mu_e\,|Y_{\lambda 0}\,|\,1s_\mu\rangle\}$$

$$\mathbf{J}=\sqrt{4\pi i}\{\mathbf{J}_{-1}+\mathbf{J}_0+\mathbf{J}_{+1}\}$$

$$\mathbf{J}_{-1}=-\sum_{\substack{\lambda=1,\ldots\\ \mu=0,\pm1}}(i)^{\lambda-1}\sqrt{\frac{2\lambda-1}{\lambda}}\begin{pmatrix}\lambda-1 & 1 & \lambda\\ 0 & \mu & -\mu\end{pmatrix}\int_0^\infty drr^2 j_{\lambda-1}(Pr)\mathbf{e}_\mu$$
$$\times\{[(\kappa_e+1)(f_{\kappa_e}g_1+g_{\kappa_e}f_1)-\lambda(g_{\kappa_e}f_1-f_{\kappa_e}g_1)]\langle\kappa_e\mu_e\,|Y_{\lambda-\mu}|-1s_\mu\rangle$$
$$-i[(\kappa_e-1)(f_{\kappa_e}f_1-g_{\kappa_e}g_1)+\lambda(g_{\kappa_e}g_1+f_{\kappa_e}f_1)]\langle\kappa_e\mu_e\,|Y_{\lambda-\mu}|\,1s_\mu\rangle\}$$

$$\mathbf{J}_0=\sum_{\substack{\lambda=1,\ldots\\ \mu=0,\pm1}}(i)^\lambda\frac{2\lambda+1}{\sqrt{\lambda(\lambda+1)}}\begin{pmatrix}\lambda & 1 & \lambda\\ 0 & \mu & -\mu\end{pmatrix}\int_0^\infty drr^2 j_\lambda(Pr)\mathbf{e}_\mu$$
$$\times\{(\kappa_e-1)(f_{\kappa_e}g_1+g_{\kappa_e}f_1)\langle-\kappa_e\mu_e\,|Y_{\lambda-\mu}|-1s_\mu\rangle$$
$$-i(\kappa_e+1)(f_{\kappa_e}f_1-g_{\kappa_e}g_1)\langle-\kappa_e\mu_e\,|Y_{\lambda-\mu}|-1s_\mu\rangle\}$$

$$\mathbf{J}_{+1}=-\sum_{\substack{\lambda=0,\mu=0\\ \lambda=1,\ldots,\mu=0\pm1}}(i)^{\lambda+1}\sqrt{\frac{2\lambda+3}{\lambda+1}}\begin{pmatrix}\lambda+1 & 1 & \lambda\\ 0 & \mu & -\mu\end{pmatrix}\int_0^\infty drr^2 j_{\lambda+1}(Pr)\mathbf{e}_\mu$$
$$\times\{[(\kappa_e+1)(f_{\kappa_e}g_1+g_{\kappa_e}f_1)+(\lambda+1)(g_{\kappa_e}f_1-f_{\kappa_e}g_1)]\langle\kappa_e\mu_e\,|Y_{\lambda-\mu}|-1s_\mu\rangle$$
$$-i[(\kappa_e-1)(f_{\kappa_e}f_1-g_{\kappa_e}g_1)-(\lambda+1)(g_{\kappa_e}g_1+f_{\kappa_e}f_1)]\langle\kappa_e\mu_e\,|Y_{\lambda-\mu}|\,1s_\mu\rangle\}$$

with $r=|\mathbf{r}|$ and $Pr=|\mathbf{P}|\,|\mathbf{r}|$.

The result of the angular matrix element $\langle \kappa_f \mu_f | Y_{\lambda\mu} | \kappa_i \mu_i \rangle$ is given in appendix C. The formula (7) was already given by Hänggi et al. [13], but it can be remarkably simplified: Using the triangle relation of the $3j$ symbols in the angular matrix elements, the summations over μ_e and s_μ can be performed:

$$\frac{d\Gamma^{V-A}(\mu^- + Z \to e^- + Z + \bar{\nu}_e + \nu_\mu)}{dE_e}$$

$$= \frac{g_{VA}^2 m_\mu}{3(2\pi)^3} \sum_{\kappa^e} \int_0^{P^{\max}} dP P^2 \{(P_0^2 - P^2) X_{\kappa_e}(P, E_e) + P^2 Y_{\kappa_e}(P, E_e) + 2P_0 P Z_{\kappa_e}(P, E_e)\} \quad (8)$$

with

$$X_{\kappa_e}(P, E_e) = \frac{2k}{(2k-1)^2} \left\{ \left(\frac{2k-1}{k-1} |(A_{-1})_{\kappa_e}|^2 + \frac{(2k-1)^2}{k(k-1)} |(A_0)_{\kappa_e}|^2 \right.\right.$$
$$\left.\left. + \frac{k-1}{k} |(A_{+1})_{\kappa_e}|^2 \right)(1 - \delta_{1,k}) + |(A_{+1})_{\kappa_e}|^2 \right\}$$
$$+ \frac{2k}{(2k+1)} \left\{ \frac{1}{k} |(B_{-1})_{\kappa_e}|^2 + \frac{(2k+1)}{k(k+1)} |(B_0)_{\kappa_e}|^2 + \frac{1}{k+1} |(B_{+1})_{\kappa_e}|^2 \right\}$$

$$Y_{\kappa_e}(P, E_e) = 2k \left\{ |(\alpha_0)_{\kappa_e}|^2 + |(\beta_0)_{\kappa_e}|^2 + \frac{1}{(2k-1)^2} |(A_{+1})_{\kappa_e} - (1 - \delta_{1,k})(A_{-1})_{\kappa_e}|^2 \right.$$
$$\left. + \frac{1}{(2k+1)^2} |(B_{+1})_{\kappa_e} - (B_{-1})_{\kappa_e}|^2 \right\}$$

$$Z_{\kappa_e}(P, E_e) = 2k Im \left\{ \frac{(\beta_0)_{\kappa_e}}{2k+1} \{(B_{+1}^*)_{\kappa_e} - (B_{-1}^*)_{\kappa_e}\} - \frac{(\alpha_0)_{\kappa_e}}{2k-1} \{(A_{+1}^*)_{\kappa_e} - (1 - \delta_{1,k})(A_{-1}^*)_{\kappa_e}\} \right\},$$

where $k = |\kappa_e|$. The functions $(A_{0,\pm1})_{\kappa_e}$, $(B_{0,\pm1})_{\kappa_e}$, $(\alpha_0)_{\kappa_e}$ and $(\beta_0)_{\kappa_e}$ are defined in Table 1.

The expression (8) does not include the recoil 4-momentum of the nucleus. Hänggi et al. [13] have proposed to include this quite complicated effect in the following manner: calculate in a first step the BOMES in Born approximation, once without inclusion of the nuclear recoil and once with inclusion. In a next state form the ratio of Bomes including to BOMES excluding the nuclear recoil. With this ratio, called recoil factor, the expression (8) has to be multiplied in order to get an energy spectrum including the nuclear recoil. Next we calculate the BOMES in Born approximation excluding the nuclear recoil effect.

BOMES in Born approximation excluding nuclear recoil

We assume that the initial muon is described by a nonrelativistic ls wave function and that there is no final state interaction between the nucleus and the outgoing electron, i.e. the electron wave function is a Dirac plane wave. Because of misprints in formula (13) of Ref. [13] we give the result of this calculation once

Table 1
Functions $(A_{0,\pm1})_{\kappa_e}$, $(B_{0,\pm1})_{\kappa_e}$, $(\alpha_0)_{\kappa_e}$ and $(\beta_0)_{\mu_e}$ used in equation (8).

$k=\lvert\kappa_e\rvert$	$\kappa_e>0$	$\kappa_e<0$
$(A_{-1})_{\kappa_e}$	$\int drr^2 j_{k-2}(Pr)\{2(1-k)f_k f_1\}$	$-i\int drr^2 j_{k-2}(Pr)\{2(1-k)g_k f_1\}$
$(A_0)_{\kappa_e}$	$\int drr^2 j_{k-1}(Pr)\{(1-k)(f_k g_1+g_k f_1)\}$	$i\int drr^2 j_{k-1}(Pr)\{(1-k)(f_k f_1-g_k g_1)\}$
$(A_{+1})_{\kappa_e}$	$\int drr^2 j_k(Pr)\{(1-2k)g_k g_1-f_k f_1\}$	$-i\int drr^2 j_k(Pr)\{(2k-1)f_k g_1-g_k f_1\}$
$(\alpha_0)_{\kappa_e}$	$-i\int drr^2 j_{k-1}(Pr)\{g_k f_1-f_k g_1\}$	$\int drr^2 j_{k-1}(Pr)\{g_k g_1+f_k f_1\}$
$(B_{-1})_{\kappa_e}$	$\int drr^2 j_{k-1}(Pr)\{(2k+1)f_k g_1+g_k f_1\}$	$-i\int drr^2 j_{k-1}(Pr)\{(2k+1)g_k g_1-f_k f_1\}$
$(B_0)_{\kappa_e}$	$\int drr^2 j_k(Pr)\{(1+k)(g_k g_1-f_k f_1)\}$	$i\int drr^2 j_k(Pr)\{(1+k)(f_k g_1+g_k f_1)\}$
$(B_{+1})_{\kappa_e}$	$-\int drr^2 j_{k+1}(Pr)\{2(k+1)g_k f_1\}$	$-i\int drr^2 j_{k+1}(Pr)\{2(k+1)f_k f_1\}$
$(\beta_0)_{\kappa_e}$	$-i\int drr^2 j_k(Pr)\{g_k g_1+f_k f_1\}$	$\int drr^2 j_k(Pr)\{f_k g_1-g_k f_1\}$

again:

$$\left.\frac{d\Gamma^{V-A}(\mu^-+Z\to e^-+Z+\bar{\nu}_e+\nu_\mu)}{dE_e}\right|_{\substack{\text{Born without}\\ \text{nuclear recoil}}}=\frac{2^4(Z\alpha m_\mu)^5 g_{VA}^2}{3^2\pi(2\pi)^3}E_e m_\mu$$
$$\times\left\{3P_0^2\{I_2^-(x)-I_2^+(x)\}+I_1^+(x)-I_1^-(x)+\frac{2P_0 p_e}{E_e}\{I_3^-(x)+I_3^+(x)\}\right.$$
$$\left.-\frac{P_0}{2E_e}\{I_4^-(x)-I_4^+(x)\}\right\}_{x=0}^{x=P^{\max}} \tag{9}$$

where

$$I_1^\pm(x)=-\left\{\left(x^2+\frac{ab^\pm x}{\Delta}+\frac{2a^2}{\Delta}\right)\frac{1}{2(R^\pm)^2}+\frac{3ab^\pm}{2\Delta}\left(\frac{b^\pm+2x}{\Delta R^\pm}+\frac{4}{\Delta^{3/2}}\operatorname{arctg}\frac{b^\pm+2x}{\Delta^{1/2}}\right)\right\}$$

$$I_2^\pm(x)=-\left\{\frac{2a+b^\pm x}{2\Delta(R^\pm)^2}+\frac{3b^\pm(b^\pm+2x)}{2\Delta^2 R^\pm}+\frac{6b^\pm}{\Delta^{5/2}}\operatorname{arctg}\frac{b^\pm+2x}{\Delta^{1/2}}\right\}$$

$$I_3^\pm(x)=\left\{\frac{ab^\pm+(b^{\pm2}-2a)x}{2\Delta(R^\pm)^2}+\frac{(2a+b^{\pm2})(-b^\pm+2x)}{2\Delta^2(R^\pm)}+\frac{4a+2b^{\pm2}}{\Delta^{5/2}}\operatorname{arctg}\frac{b^\pm+2x}{\Delta^{1/2}}\right\}$$

$$I_4^\pm(x)=-\left\{\frac{2a+b^\pm x}{\Delta R^\pm}+\frac{2b^\pm}{\Delta^{3/2}}\operatorname{arctg}\frac{b^\pm+2x}{\Delta^{1/2}}\right\}$$

with

$$a=(Z\alpha m_\mu)^2+p_e^2,\qquad b^\pm=\pm2p_e,\qquad \Delta=(2Z\alpha m_\mu)^2,$$
$$R^\pm=a+b^\pm x+x^2\quad\text{and}\quad p_e=|\mathbf{p}_e|.$$

In order to calculate the recoil factor $R_{(V-A)}(E_e)$ we have to evaluate the BOMES in Born approximation including nuclear recoil.

BOMES in Born approximation including nuclear recoil

Treating the motion of the recoiling nucleus nonrelativistically our starting equation is

$$\begin{aligned}\frac{d^{(1)}W_{V-A}}{dt} &= \frac{g_{VA}^2}{(2\pi)^5}\, d^3p_e \int d^3p_Z^f \int \frac{d^3k_e}{E_{\bar{\nu}_e}} \int \frac{d^3k_\mu}{E_{\nu_\mu}} \\ &\times\{J_{VA}^{\lambda}(p_e, \mathbf{s}_e, B_{1s_{1/2}}, \rho(\mathbf{p}_\mu), \mathbf{s}_\mu, \mathbf{P}) J_{VA}^{\varphi *}(p_e, \mathbf{s}_e, B_{1s_{1/2}}, \rho(\mathbf{p}_\mu), \mathbf{s}_\mu, \mathbf{P})\} \\ &\times\{(k_e)_\lambda (k_\mu)_\varphi + (k_\mu)_\lambda (k_e)_\varphi - g_{\lambda\varphi}(k_\mu k_e) \\ &+ i(k_\mu)^\mu (k_e)^\nu \varepsilon_{\lambda\mu\varphi\nu}\}\, \delta^{(4)}(p_\mu + p_Z^i - p_e - k_e - k_\mu - p_Z^f) \end{aligned} \tag{10}$$

where $p_Z^{i,f}$ is the four-momentum of the nucleus in the intital (i) and final (f) state, respectively. Evaluating the two neutrino three-momentum integrations one gets

$$\begin{aligned}\left.\frac{d\Gamma^{V-A}(\mu^- + Z \to e^- + Z + \bar{\nu}_e + \nu_\mu)}{dE_e}\right|_{\substack{\text{Born with}\\ \text{nuclear recoil}}} &= \frac{g_{VA}^2 C_\mu^2 m_\mu}{3(2\pi)^7} |\mathbf{p}_e| \int d\Omega(\hat{\mathbf{p}}_e) \int d^3p_Z^f \left| \int d^3r e^{-i(\mathbf{p}_\mu + \mathbf{p}_Z^i - \mathbf{p}_Z^f)\mathbf{r}} e^{-Z\alpha m_\mu |\mathbf{r}|}\right|^2 \\ &\times\{p_e^\lambda p_\mu^\varphi + p_e^\varphi p_\mu^\lambda - p_e p_\mu g^{\lambda\varphi}\}\{\bar{P}_\lambda \bar{P}_\varphi - \bar{P}^2 g_{\lambda\varphi}\} \end{aligned} \tag{11}$$

with $C_\mu = (Z\alpha m_\mu)^{3/2}/\pi^{1/2}$ and $\bar{P} = p_Z^i - (p_Z^f + p_e)$.

If we put $\mathbf{p}_Z^i + \mathbf{p}_\mu = 0$ and $(p_\mu)_0 + (p_Z^i)_0 = E_\mu + M_Z$, we arrive after performing the two solid angle integrations at the final result:

$$\left.\frac{d\Gamma^{V-A}(\mu^- + Z \to e^- + Z + \bar{\nu}_e + \nu_\mu)}{dE_e}\right|_{\substack{\text{Born with}\\ \text{nuclear recoil}}} = \frac{2^5 (Z\alpha m_\mu)^5 g_{VA}^2}{3\pi(2\pi)^3} p_e E_e m_\mu \begin{cases} f_1(E_e) \\ f_2(E_e) \end{cases} \text{for} \quad E_e \begin{Bmatrix} \leqslant \\ \geqslant \end{Bmatrix} \frac{1+E_\mu^2}{2E_\mu} \tag{12}$$

with $p_e = |\mathbf{p}_e|$, $p_Z^f = |\mathbf{p}_Z^f|$ and

$$f_1(E_e) = \int_0^{x_1} \frac{2a(p_Z^f)^2 dp_Z^f}{[(Z\alpha m_\mu)^2 + (p_Z^f)^2]^4} + \int_{x_1}^{x_2} \frac{(p_Z^f)^2\, dp_Z^f}{[(Z\alpha m_\mu)^2 + (p_Z^f)^2]^4} \left\{a(\varphi+1) + \frac{b}{2}(\varphi^2 - 1)\right\}$$

$$f_2(E_e) = \int_{x_3}^{x_2} \frac{(p_Z^f)^2 dp_Z^f}{[(Z\alpha m_\mu)^2 + (p_Z^f)^2]^4} \left\{a(\varphi+1) + \frac{b}{2}(\varphi^2 - 1)\right\}$$

$$a = 3\bar{P}_0^2 - (p_Z^f)^2 - p_e^2 + \frac{2\bar{P}_0}{E_e} p_e^2, \qquad b = 2\left(\frac{\bar{P}_0}{E_e} - 1\right) p_e p_Z^f, \qquad \bar{P}_0 = E_\mu - E_e - \frac{(p_Z^f)^2}{2M_Z}$$

$$\alpha = 1 + \frac{E_\mu - E_e}{M_Z}. \qquad \beta = 2p_e, \qquad \gamma = p_e^2 - (E_\mu - E_e)^2, \qquad \varphi = -\frac{1}{\beta}\left(\alpha p_Z^f + \frac{\gamma}{p_Z^f}\right)$$

$$x_{\substack{1\\2\\3}} = \frac{\mp\beta \pm \sqrt{\beta^2 - 4\alpha\gamma}}{2\alpha},$$

M_Z is the mass of the nucleus with charge number Z.

We define the $(V-A)$ recoil factor $R_{(V-A)}(E_e)$ as the ratio of equation (12) and equation (9). In order to eliminate the coupling constant g_{VA} we normalize equation (8) by the free decay rate

$$\Gamma^{V-A}(\mu^- \to e^- + \bar{\nu}_e + \nu_\mu) = \frac{g_{VA}^2 m_\mu^5}{3 \cdot 2^3 (2\pi)^3} \tag{13}$$

The final result for the BOMES, resulting from bound muon decay via $(V-A)$ interaction including the nuclear recoil is

$$\frac{d\Gamma^{V-A}(\mu^- + Z \to e^- + Z + \bar{\nu}_e + \nu_\mu)}{dE_e} = R_{(V-A)}(E_e)\Gamma^{V-A}(\mu^- \to e^- + \bar{\nu}_e + \nu_\mu)\frac{2^3}{m_\mu}$$
$$\times \sum_{\kappa_e} \int_0^{P_{max}} dP P^2 \{(P_0^2 - P^2) X_{\kappa_e}(P, E_e) + P^2 Y_{\kappa_e}(P, E_e) + 2P_0 P Z_{\kappa_e}(P, E_e)\} \tag{14}$$

where the functions $X_{\kappa_e}(P, E_e)$, $Y_{\kappa_e}(P, E_e)$ and $Z_\kappa(P, E_e)$ are given in equation (8).

II.2 *Bound muon electron spectra assuming S- and P-interaction*

All the arguments used for the calculation of the $(V-A)$ BOMES are also applicable in this case. Therefore, we do not repeat all steps done earlier, but give directly the results:

$$\frac{d\Gamma^s(\mu^- + Z \to e^- + Z + \bar{\nu}_e + \nu_\mu)}{dE_e} = R_s(E_e)\Gamma^s(\mu^- \to e^- + \bar{\nu}_e + \nu_\mu)\frac{3 \cdot 2^6}{m_\mu^3(m_\mu + 4)}$$
$$\times \left\{ \sum_{\kappa_e > 0} \kappa_e \int_0^{P_{max}} dP P^2 (P_0^2 - P^2) \left| \int_0^\infty dr r^2 j_{\kappa_e}(Pr)\{g_{\kappa_e} g_1 - f_{\kappa_e} f_1\} \right|^2 \right.$$
$$\left. + \sum_{\kappa_e < 0} |\kappa_e| \int_0^{P_{max}} dP P^2 (P_0^2 - P^2) \left| \int_0^\infty dr r^2 j_{|\kappa_e|-1}(Pr)\{g_{\kappa_e} g_1 - f_{\kappa_e} f_1\} \right|^2 \right\} \tag{15}$$

where

$$\Gamma^s(\mu^- \to e^- + \bar{\nu}_e + \nu_\mu) = \frac{g_s^2 m_\mu^4 (m_\mu + 4)}{3 \cdot 2^7 (2\pi)^3}$$

and $R_s(E_e)$ is the S recoil factor defined by analogy with $R_{(V-A)}(E_e)$.

For completeness we give here the formulae relevent for the determination of $R_s(E_e)$, using the same arguments as in the $(V-A)$ interaction case:

$$\left. \frac{d\Gamma^s(\mu^- + Z \to e^- + Z + \bar{\nu}_e + \nu_\mu)}{dE_e} \right|_{\substack{\text{Born without} \\ \text{nuclear recoil}}}$$
$$= \frac{2(Z\alpha m_\mu)^5 g_s^2}{3\pi(2\pi)^3}(E_e + 1) m_\mu \{P_0^2\{I_2^-(x) - I_2^+(x)\} + I_1^+(x) - I_1^-(x)\}_{x=0}^{P_{max}} \tag{16}$$

The functions $I_1^{\pm}(x)$ and $I_2^{\pm}(x)$ are defined in equation (9). For the Born BOMES including the nuclear recoil we get:

$$\left.\frac{d\Gamma^s(\mu^- + Z \to e^- + Z + \bar{\nu}_e + \nu_\mu)}{dE_e}\right|_{\substack{\text{Born with}\\ \text{nuclear recoil}}}$$

$$= \frac{2^2(Z\alpha m_\mu)^5 g_s^2}{\pi(2\pi)^3} p_e(E_e+1)m_\mu \begin{cases} f_1(E_e) \\ f_2(E_2) \end{cases} \quad \text{for} \quad E_e \begin{Bmatrix} \leqslant \\ \geqslant \end{Bmatrix} \frac{1+E_\mu^2}{2E_\mu} \tag{17}$$

where the functions $f_1(E_e)$ and $f_2(E_e)$ are the same as in equation (12), but the expressions for a and b must be changed as follows

$$a = \bar{P}_0^2 - p_e^2 - (p_Z^f)^2, \qquad b = -2p_e p_Z^f.$$

The recoil factor $R_s(E_e)$ is now given as the ratio of the result of equation (17) and equation (16).
The P interaction leads to the following expression for the BOMES:

$$\frac{d\Gamma^P(\mu^- + Z \to e^- + Z + \bar{\nu}_e + \nu_\mu)}{dE_e} = R_s(E_e)\Gamma^P(\mu^- \to e^- + \bar{\nu}_e + \nu_\mu)\frac{3\cdot 2^6}{m_\mu^3(m_\mu - 4)}$$

$$\times \left\{ \sum_{\kappa_e > 0} \kappa_e \int_0^{P^{\max}} dP P^2(P_0^2 - P^2) \left| \int_0^\infty dr r^2 j_{\kappa_e - 1}(Pr)\{g_{\kappa_e} f_1 + f_{\kappa_e} g_1\} \right|^2 \right.$$

$$\left. + \sum_{\kappa_e < 0} |\kappa_e| \int_0^{P^{\max}} dP P^2(P_0^2 - P^2) \left| \int_0^\infty dr r^2 j_{|\kappa_e|}(Pr)\{g_{\kappa_e} f_1 + f_{\kappa_e} g_1\} \right|^2 \right\} \tag{18}$$

The free decay rate $\Gamma^P(\mu^- \to e^- + \bar{\nu}_e + \nu_\mu)$ is given by

$$\Gamma^P(\mu^- \to e^- + \bar{\nu}_e + \nu_\mu) = \frac{g_P^2 m_\mu^2(m_\mu - 4)}{3\cdot 2^7(2\pi)^3}.$$

In formula (18) we have used the fact that $R_p(E_e)$ and $R_s(E_e)$ are equal up to the order of 10^{-8} in the entire energy range.

II.3. *Bound muon electron spectrum assuming T-interaction*

In this case equation (5) results in

$$\frac{d^{(1)}W_T}{dt} = \frac{g_T^2}{2^2(2\pi)^8}\frac{d^3p_e}{E_e}\int\frac{d^3k_e}{E_{\bar{\nu}_e}}\int\frac{d^3k_\mu}{E_{\nu_\mu}}$$

$$\times J_T^{\alpha\beta}(p_e, \mathbf{s}_e, B_{1s_{1/2}}, \rho(\mathbf{p}_\mu), \mathbf{s}_\mu, \mathbf{P}) J_T^{\lambda\delta *}(p_e, \mathbf{s}_e, B_{1s_{1/2}}, \rho(\mathbf{p}_\mu), \mathbf{s}_\mu, \mathbf{P})$$

$$\times \{(k_\mu)_\alpha\{(k_e)_\lambda g_{\beta\delta} - (k_e)_\delta g_{\beta\lambda}\} - (k_\mu)_\beta\{(k_e)_\lambda g_{\alpha\delta} - (k_e)_\delta g_{\alpha\lambda}\} + (k_e k_\mu)$$

$$\times \{g_{\alpha\delta}g_{\beta\lambda} - g_{\alpha\lambda}g_{\beta\delta}\} - (k_\mu)_\lambda\{(k_e)_\beta g_{\alpha\delta} - (k_e)_a g_{\beta\delta}\}$$

$$+ (k_\mu)_\delta\{(k_e)_\beta g_{\alpha\lambda} - (k_e)_\alpha g_{\beta\lambda}\}\}\delta(E_\mu - E_e - E_{\bar{\nu}_e} - E_{\nu_\mu}) \tag{19}$$

Table 2
Expressions A_{κ_e}, B_{κ_e}, C_{κ_e}, D_{κ_e} and E_{κ_e} used in equation (19).

$k=\lvert\kappa_e\rvert$	$\kappa_e>0$	$\kappa_e<0$
A_{κ_e}	$2k\left\{\frac{1}{2k+1}\left\{\frac{(G^{-1})^2}{k}+\frac{(G^{+1})^2}{k+1}\right\}+\frac{(1-\delta_{1,k})}{k(k-1)}(G^0)^2\right\}$	$2k\left\{\frac{1}{2k-1}\left\{\frac{(G^{-1})^2}{k-1}(1-\delta_{1,k})+\frac{((1-\delta_{1,k})(k-1)+k)}{2k-1}\frac{(G^{+1})^2}{k}+\frac{(G^0)^2}{k(k+1)}\right\}\right.$
B_{κ_e}	$2k\left\{\frac{1}{2k-1}\left\{\frac{(F^{-1})^2}{k-1}(1-\delta_{1,k})+\frac{((1-\delta_{1,k})(k-1)+k)}{2k-1}\frac{(F^{+1})^2}{k}+\frac{(F^0)^2}{k(k+1)}\right\}\right.$	$2k\left\{\frac{1}{2k+1}\left\{\frac{(F^{-1})^2}{k}+\frac{(F^{+1})^2}{k+1}\right\}+\frac{(1-\delta_{1,k})}{k(k-1)}(F^0)^2\right\}$
C_{κ_e}	$2k\frac{(G^{-1}+G^{+1})^2}{(2k+1)^2}$	$2k\left\{\frac{1}{(2k-1)^2}\{(1-\delta_{1,k})G^{-1}+G^{+1}\}^2\right\}$
D_{κ_e}	$2k\left\{\frac{1}{(2k-1)^2}\{(1-\delta_{1,k})F^{-1}+F^{+1}\}^2\right\}$	$2k\frac{(F^{-1}+F^{+1})^2}{(2k+1)^2}$
E_{κ_e}	$2k\left\{\frac{1}{2k+1}\left\{\frac{G^{-1}}{k}-\frac{G^{+1}}{k+1}\right\}F^0+\frac{(1-\delta_{1,k})}{2k-1}\left\{\frac{F^{+1}}{k}-\frac{F^{-1}}{k-1}\right\}G^0\right\}$	$2k\left\{\frac{1}{2k+1}\left\{\frac{F^{+1}}{k+1}-\frac{F^{-1}}{k}\right\}G^0+\frac{(1-\delta_{1,k})}{2k-1}\left\{\frac{G^{-1}}{k-1}-\frac{G^{+1}}{k}\right\}F^0\right\}$

Doing analogue steps as in the former cases we find:

$$\frac{d\Gamma^{\mathrm{T}}(\mu^- + Z \to e^- + Z + \bar{\nu}_e + \nu_\mu)}{dE_e} = R_{\mathrm{T}}(E_e)\Gamma^{\mathrm{T}}(\mu^- \to e^- + \bar{\nu}_e + \nu_\mu)\frac{2^4}{3 \cdot m_\mu^4}$$

$$\times \sum_{\kappa_e} \int_0^{P^{\max}} dPP^2\{(P_0^2 + P^2)\{A_{\kappa_e} + B_{\kappa_e}\} - 2P^2\{C_{\kappa_e} + D_{\kappa_e}\} + 4P_0PE_{\kappa_e}\} \quad (20)$$

where the functions A_{κ_e}, B_{κ_e}, C_{κ_e}, D_{κ_e} and E_{κ_e} are given in Table 2. The functions G and F are defined in Table 3.

In formula (20) $\Gamma^{\mathrm{T}}(\mu^- \to e^- + \bar{\nu}_e + \nu_\mu)$ is given by

$$\Gamma^{\mathrm{T}}(\mu^- \to e^- + \bar{\nu}_e + \nu_\mu) = \frac{g_{\mathrm{T}}^2 m_\mu^5}{2^4(2\pi)^3}.$$

The recoil factor $R_{\mathrm{T}}(E_e)$ can be calculated with the help of the two following expressions:

$$\left.\frac{d\Gamma^{\mathrm{T}}(\mu^- + Z \to e^- + Z + \bar{\nu}_e + \nu_\mu)}{dE_e}\right|_{\substack{\text{Born without}\\ \text{nuclear recoil}}} = \frac{2^4(Z\alpha m_\mu)^5 g_{\mathrm{T}}^2}{3^2\pi(2\pi)^3} E_e m_\mu \Big\{3P_0^2\{I_2^-(x) \quad (21)$$

$$- I_2^+(x)\} + I_1^-(x) - I_1^+(x) + \frac{4P_0p_e}{E_e}\{I_3^-(x) + I_3^+(x)\} - \frac{P_0}{E_e}\{I_4^-(x) - I_4^+(x)\}\Big\}_{x=0}^{x=P^{\max}}$$

The functions $I_i^{\pm}(x)$, $i = 1, \ldots, 4$ are the same as in equation (9).

$$\left.\frac{d\Gamma^{\mathrm{T}}(\mu^- + Z \to e^- + Z + \bar{\nu}_e + \nu_\mu)}{dE_e}\right|_{\substack{\text{Born with}\\ \text{nuclear recoil}}}$$

$$= \frac{2^5(Z\alpha m_\mu)^5 g_{\mathrm{T}}^2}{3\pi(2\pi)^3} p_e E_e m_\mu \begin{cases} f_1(E_e) \\ f_2(E_e) \end{cases} \text{for} \quad E_e \begin{Bmatrix} \leqslant \\ \geqslant \end{Bmatrix} \frac{1 + E_\mu^2}{2E_\mu} \quad (22)$$

Table 3
Functions $G^{0,\pm1}$ and $F^{0,\pm1}$ used in the expressions of Table 2.

$k = \lvert\kappa_e\rvert$	$\kappa_e > 0$	$\kappa_e < 0$
G^{-1}	$\int drr^2 j_{k-1}(Pr)\{(2k+1)f_k g_1 - {}_k f_1\}$	$2(k-1)\int drr^2 j_{k-2}(Pr)\{g_k f_1\}$
G^0	$\int drr^2 j_{k-1}(Pr)\{(k-1)(g_k f_1 - f_k g_1)\}$	$\int drr^2 j_k(Pr)\{(k+1)(f_k g_1 - g_k f_1)\}$
G^{+1}	$-2(k+1)\int drr^2 j_{k+1}(Pr)\{g_k f_1\}$	$-\int drr^2 j_k(Pr)\{(2k-1)f_k g_1 + g_k f_1\}$
F^{-1}	$-2(k-1)\int drr^2 j_{k-2}(Pr)\{f_k f_1\}$	$\int drr^2 j_{k-1}(Pr)\{(2k+1)g_k g_1 + f_k f_1\}$
F^0	$\int drr^2 j_k(Pr)\{(k+1)(g_k g_1 + f_k f_1)\}$	$-\int drr^2 j_{k-1}(Pr)\{(k-1)(g_k g_1 + f_k f_1)\}$
F^{+1}	$-\int drr^2 j_k(Pr)\{(2k-1)g_k g_1 - f_k f_1\}$	$2(k+1)\int drr^2 j_{k+1}(Pr)\{f_k f_1\}$

The functions $f_1(E_e)$ and $f_2(E_e)$ are still the same as in equation (12), but the expressions for a and b are given now by

$$a = 3\bar{P}_0^2 + (p_Z^f)^2 - p_e^2 + \frac{4\bar{P}}{E_e} p_e^2, \qquad b = 2\left(\frac{2\bar{P}_0}{E_e} + 1\right) p_e p_Z^f$$

III. Numerical results

For the numerical evaluation of the BOMES (equations (14), (15), (18) and (20)) we have chosen the following procedure:

- Calculation of the electron- and muon-wave functions (appendix B).
- Calculation of the spherical bessel functions $j_l(Pr)$ by means of well-known recursion relations [14].
- Evaluation of the radial integrals.
- Integration over momentum transfer P.
- Summation over κ_e: The summation procedure has been finished at the point, where the amount of relative increase was smaller than 10^{-5}.
- Determination of the recoil factors $R_i(E_e)$, where i is the coupling type index.

In Table 4–Table 9 we present decay electron spectra of various muonic atoms which are of some importance for present or future muon electron

Table 4
Decay electron energy spectra of ^{nat}Mg ($c = 3.045$ fm, $t = 2$, 3 fm).

E_e^{tot} [a]	$V-A$ [b]	S [c]	P [d]	T [e]
10	1.249-01	2.575-01	2.213-01	8.659-02
20	4.382-01	8.277-01	7.824-01	3.158-01
30	8.814-01	1.555	1.517	6.631-01
40	1.410	2.311	2.289	1.113
50	1.981	2.967	2.967	1.652
60	2.549	3.395	3.415	2.264
70	3.068	3.463	3.500	2.931
80	3.487	3.047	3.090	3.627
90	3.706	2.040	2.074	4.256
100	2.683	5.859-01	5.966-01	3.380
110	1.751-01	2.244-02	2.286-02	2.259-01
120	6.056-03	8.555-04	8.715-04	7.787-03
130	4.440-04	6.389-05	6.512-05	5.705-04
140	5.008-05	6.580-06	6.711-06	6.457-05
150	6.846-06	7.476-07	7.631-07	8.878-06
160	9.704-07	8.012-08	8.185-08	1.267-06
170	1.237-07	6.882-09	7.037-09	1.626-07
180	1.158-08	3.683-10	3.769-10	1.532-08
190	5.112-10	6.935-12	7.097-12	6.794-10
200	1.632-12	4.412-15	4.505-15	2.169-12

a) E_e^{tot}: Total energy of the electron in units of $[m_e]$.
b) $V-A$: BOMES according to equation (14).
c) S: BOMES according to equation (15).
d) P: BOMES according to equation (18).
e) T: BOMES according to equation (20).

Table 5
Decay electron energy spectra of $^{32}_{16}S$ ($c = 3.352$ fm, $t = 2.3$ fm).

E_e^{tot} a)	$V-A$ b)	S c)	P d)	T e)
10	1.359-01	2.784-01	2.400-01	9.463-02
20	4.682-01	8.781-01	8.319-01	3.391-01
30	9.265-01	1.621	1.583	7.011-01
40	1.463	2.373	2.353	1.163
50	2.036	3.008	3.009	1.711
60	2.560	3.396	3.419	2.330
70	3.109	3.413	3.450	3.001
80	3.505	2.936	2.978	3.688
90	3.616	1.888	1.919	4.187
100	2.321	5.543-01	5.643-01	2.909
110	2.607-01	3.932-02	4.004-02	3.344-01
120	1.492-02	2.225-03	2.267-03	1.914-02
130	1.281-03	1.867-04	1.903-04	1.645-03
140	1.518-04	1.985-05	2.024-05	1.957-04
150	2.095-05	2.257-06	2.304-06	2.718-05
160	2.944-06	2.383-07	2.434-07	3.845-06
170	3.670-07	1.992-08	2.037-08	4.827-07
180	3.309-08	1.021-09	1.045-09	4.378-08
190	1.355-09	1.775-11	1.816-11	1.801-09
200	3.184-12	8.293-15	8.463-15	4.236-12

The meaning of the colums a), . . . , e) is the same as in Table 4.

Table 6
Decay electron energy spectra of $^{nat}_{18}Ar$ ($c = 3.625$ fm, $t = 2.3$ fm).

E_e^{tot} a)	$V-A$ b)	S c)	P d)	T e)
10	1.418-01	2.896-01	2.501-01	9.902-02
20	4.846-01	9.052-01	8.586-01	3.520-01
30	9.515-01	1.657	1.620	7.225-01
40	1.493	2.407	2.388	1.192
50	2.066	3.028	3.031	1.745
60	2.626	3.393	3.417	2.367
70	3.127	3.378	3.415	3.037
80	3.501	2.865	2.906	3.707
90	3.534	1.801	1.831	4.107
100	2.159	5.342-01	5.438-01	2.699
110	2.892-01	4.645-02	4.731-02	3.700-01
120	2.008-02	3.068-03	3.126-02	2.575-02
130	1.852-03	2.709-04	2.761-04	2.378-03
140	2.238-04	2.913-05	2.971-05	2.887-04
150	3.088-05	3.295-06	3.363-06	4.007-05
160	4.289-06	3.429-07	3.503-07	5.604-06
170	5.244-07	2.807-08	2.870-08	6.899-07
180	4.592-08	1.397-09	1.430-09	6.077-08
190	1.786-09	2.313-11	2.367-11	2.373-09
200	3.430-12	9.060-15	9.241-15	4.566-12

The meaning of the columns a), . . . , e) is the same as in Table 4.

Table 7
Decay electron energy spectra of $^{40}_{20}$Ca ($c = 3.720$ fm, $t = 2.3$ fm).

E_e^{tot} a)	$V-A$ b)	S c)	P d)	T e)
10	1.481-01	3.013-01	2.606-01	1.037-01
20	5.021-01	9.337-01	8.866-01	3.659-01
30	9.783-01	1.694	1.658	7.456-01
40	1.525	2.442	2.424	1.223
50	2.099	3.048	3.052	1.781
60	2.654	3.388	3.412	2.406
70	3.144	3.337	3.375	3.073
80	3.490	2.787	2.827	3.718
90	3.435	1.711	1.740	4.005
100	2.009	5.127-01	5.220-01	2.507
110	3.098-01	5.255-02	5.352-02	3.953-01
120	2.550-02	3.989-03	4.064-03	3.265-02
130	2.531-03	3.722-04	3.794-04	3.249-03
140	3.144-04	4.074-05	4.156-05	4.055-04
150	4.368-05	4.614-06	4.710-06	5.669-05
160	6.043-06	4.761-07	4.864-07	7.898-06
170	7.296-07	3.828-08	3.914-08	9.601-07
180	6.231-08	1.846-09	1.888-09	8.248-08
190	2.289-09	2.852-11	2.918-11	3.042-09
200	3.285-12	8.066-15	8.224-15	4.372-12

The meaning of the columns a), . . . , e) is the same as in Table 4.

Table 8
Decay electron energy spectra of $^{56}_{26}$Fe ($c = 4.118$ fm, $t = 2.3$ fm).

E_e^{tot} a)	$V-A$ b)	S c)	P d)	T e)
10	1.691-01	3.394-01	2.953-01	1.195-01
20	5.594-01	1.025	9.764-01	4.122-01
30	1.066	1.813	1.778	8.228-01
40	1.629	2.548	2.534	1.325
50	2.203	3.102	3.110	1.902
60	2.740	3.353	3.380	2.531
70	3.183	3.187	3.226	3.175
80	3.416	2.530	2.567	3.705
90	3.089	1.452	1.476	3.631
100	1.638	4.459-01	4.538-01	2.034
110	3.314-01	6.322-02	6.438-02	4.206-01
120	3.938-02	6.515-03	6.638-03	5.031-02
130	4.703-03	6.984-04	7.119-04	6.037-03
140	6.273-04	7.992-05	8.152-05	8.095-04
150	8.835-05	9.016-06	9.204-06	1.148-04
160	1.198-05	8.985-07	9.179-07	1.567-05
170	1.375-06	6.772-08	6.925-08	1.811-06
180	1.070-07	2.922-09	2.989-09	1.418-07
190	3.190-09	3.562-11	3.642-11	4.241-09
200	1.330-12	2.742-15	2.790-15	1.769-12

The meaning of the columns a), . . . , e) is the same as in Table 4.

Table 9
Decay electron energy spectra of $^{66}_{30}Zn$ ($c = 4$, 440 fm, $t = 2$, 3 fm).

E_e^{tot} a)	$V-A$ b)	S c)	P d	T e)
10	1.850-01	3.677-01	3.213-01	1.317-01
20	6.014-01	1.090	1.040	4.467-01
30	1.129	1.894	1.860	8.795-01
40	1.702	2.617	2.605	1.400
50	2.274	3.130	3.140	1.987
60	2.794	3.315	3.344	2.616
70	3.196	3.072	3.110	3.231
80	3.336	2.353	2.388	3.658
90	2.849	1.296	1.317	3.363
100	1.441	4.017-01	4.088-01	1.786
110	3.236-01	6.473-02	6.592-02	4.097-01
120	4.500-02	7.621-03	7.765-03	5.743-02
130	5.888-03	8.735-04	8.905-04	7.557-03
140	8.128-04	1.018-04	1.038-04	1.050-03
150	1.145-04	1.135-05	1.159-05	1.489-04
160	1.518-05	1.095-06	1.118-06	1.987-05
170	1.666-06	7.801-08	7.977-08	2.195-06
180	1.195-07	3.062-09	3.132-09	1.583-07
190	2.952-09	3.041-11	3.109-11	3.927-09
200	2.690-13	4.944-16	5.022-16	3.570-13

The meaning of the columns a), . . . , e) is the same as in Table 4.

conversion experiments (Refs [2], [9] and [10]). The decay electron energy spectra for the four different interaction types (according to equations (14), (15), (18) and (20)) are listed at twenty points in the energy range $10[m_e] \leqslant E_e \leqslant 200[m_e]$, where E_e is the total energy of the outgoing electron.

The two Fermi parameters, c and t, used for the description of the nucleus with charge distribution $\rho_F^{c,t}(r)$ are taken from Ref. [15]. There $\rho_F^{c,t}(r)$ is defined as follows:

$$\rho_F^{c,t}(r) = \frac{\rho_0}{1+\exp[(r-c)4\ln 3/t]} = \frac{\rho_0}{1+\exp[(r-c)/a]} \tag{22}$$

where a is given by $a = t/4 \ln 3$.

The normalization

$$4\pi \int dr r^2 \rho_F^{c,t}(r) = Z$$

determines ρ_0:

$$\rho_0 = \frac{3Z}{4\pi c^3}\left\{1+\left(\frac{\pi a}{c}\right)^2 - 6\left(\frac{a}{c}\right)^3 \sum_{n=1}^{\infty} (-1)^n \frac{e^{-nc/a}}{n^3}\right\}^{-1} \tag{23a}$$

IV. Estimate of the electron bremsstrahlung effect on the BOMES shape

We are looking at the bremsstrahlung graphs drawn in Fig. 3. Since the emitted electron is influenced by the nuclear Coulomb field, one may ask for the

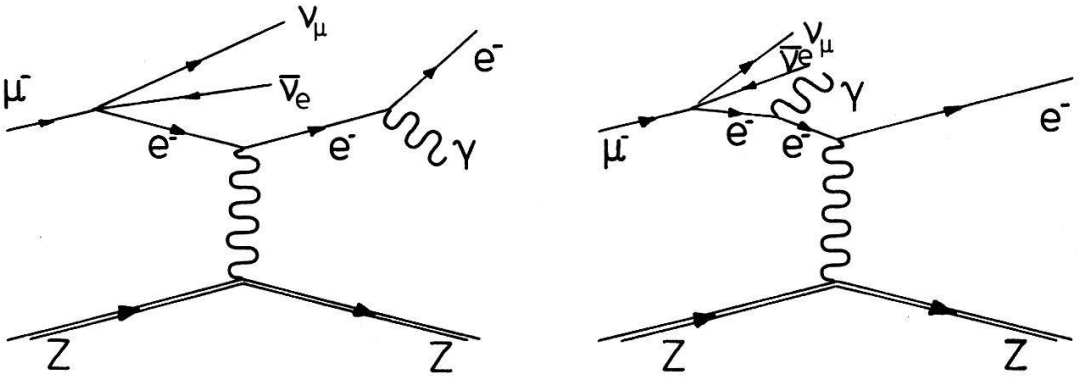

Figure 3
Bremsstrahlung graphs, which give rise to a change of the shape of the bound muon decay electron spectrum according to equation (24).

effect of the electron bremsstrahlung on the BOMES shape. We assume that the energy of an electron lies at the energy point $E_e^{(1)}$ within an interval ΔE_e, given by the experimental resolution. We determine the probability, that this electron radiates off a photon of energy $\omega > \Delta E_e$, so that the electron leaves the initial energy interval at $E_e^{(1)}$ and populates an interval at a lower energy $E_e^{(2)} \leqslant E_e^{(1)} - \Delta E_e/2$.

Taking this electron bremsstrahlung effect into account we have found for the bremsstrahlung corrected rate $\Gamma^i(E_e^{(1)})$ at point $E_e^{(1)}$ the following estimate (the index i refers to the four different interaction types, $i = (V-A), S, P, T$):

$$\Gamma^i(E_e^{(1)})\Big|_{\substack{\text{with bremsstrahlung}\\ \text{correction}}} = \Gamma^i(E_e^{(1)}) + \int_{E_e^{(1)}+\Delta E_e/2}^{m_\mu - B_{1s\,1/2}} dE_e^{(k)} \Gamma^i(E^{(k)}) \frac{1}{F} \frac{d\sigma(E_e^{(k)}, E_e^{(1)})}{dE_e^{(1)}} - \int_1^{E_e^{(1)}-\Delta E_e/2} dE_e^{(2)} \Gamma^i(E_e^{(1)}) \frac{1}{F} \frac{d\sigma(E_e^{(1)}, E_e^{(2)})}{dE_e^{(2)}} \quad (24)$$

The expression $d\sigma(E_e^{(i)}, E_e^{(f)})/dE_e^{(f)}$ is the differential cross section for emission of a bremsstrahlung quantum with energy $\omega = E_e^{(i)} - E_e^{(f)}$ from an electron of energy $E_e^{(i)}$. In the high energy limit $E_e^{(i)} \gg 1$ and $E_e^{(f)} \gg 1$ this differential cross section is given by Ref. [16] as

$$\frac{d\sigma(E_e^{(i)}, E_e^{(f)})}{dE_e^{(f)}} = \frac{4Z^2\alpha^3}{(E_e^{(i)} - E_e^{(f)})(E_e^{(i)})^2} \times \{(E_e^{(i)})^2 - (E_e^{(f)})^2 - \tfrac{2}{3}E_e^{(i)}E_e^{(f)}\}\left\{\ln(183Z^{-1/3}) + \frac{(E_e^{(i)})^2}{(E_e^{(i)})^2 - 1} f(Z\alpha) + \frac{E_e^{(i)}E_e^{(f)}}{9}\right\} \quad (25)$$

where

$$f(Z\alpha) = (Z\alpha)^2 \sum_{n=1}^{\infty} \frac{1}{n(n^2 + (Z\alpha)^2)}$$

and α is the fine structure constant. The area F, originating from the incoming particle flux, is not uniquely defined here, but the simplest area one can imagine in this context is given by the surface area of the sphere with radius $\langle r \rangle$, defined as

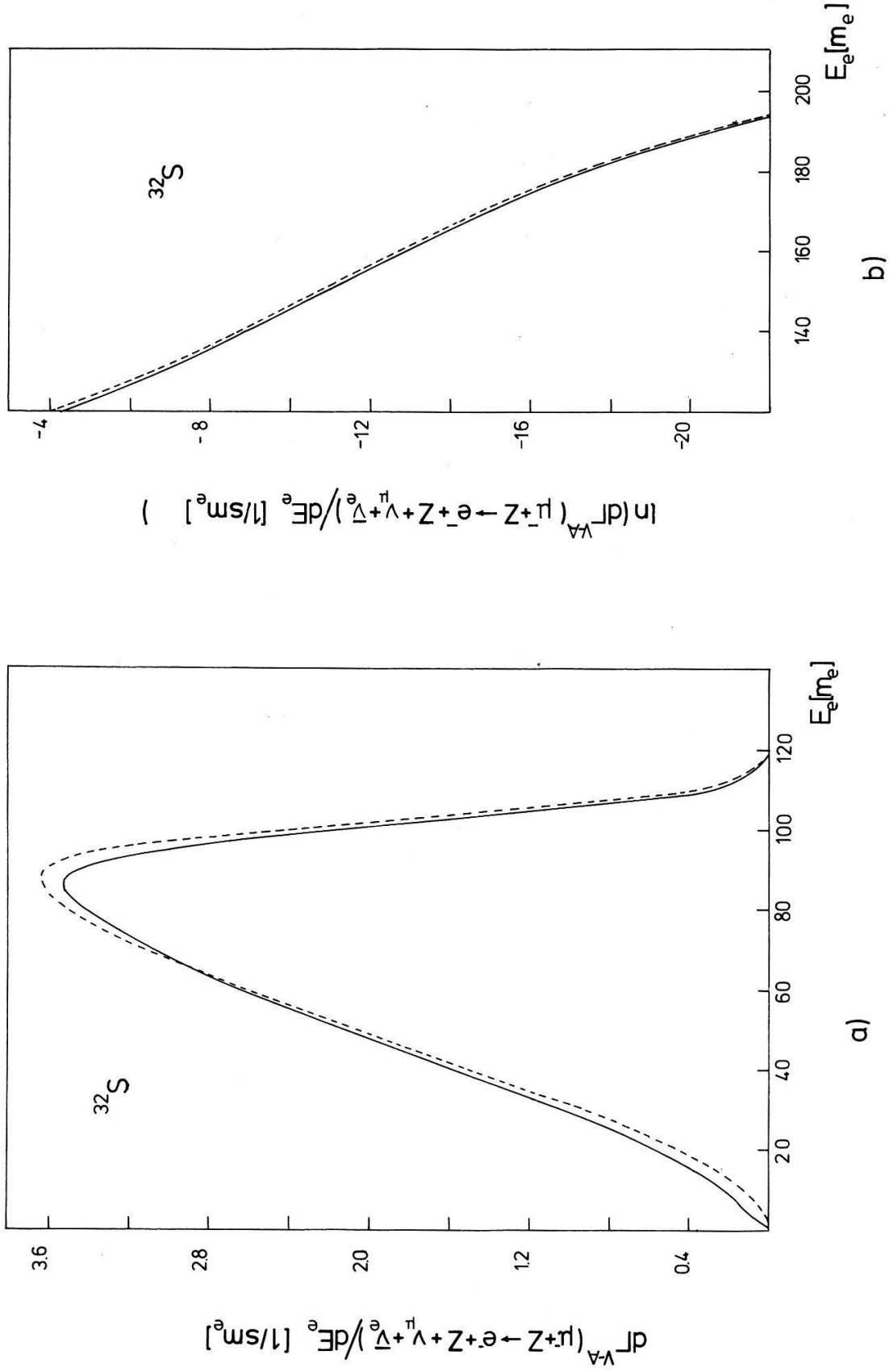

Figure 4
BOMES assuming $(V-A)$ interaction without bremsstrahlung correction (dashed line) and with maximum bremsstrahlung correction (full line) for ^{32}S.

the mean value of the $1s_{1/2}$ shell radius, the possiblest origin of the electron:

$$\langle r\rangle = \int d^3r\, |\mathbf{r}|\, \varphi_\mu^+(B_{1s_{1/2}}, \rho(\mathbf{p}_\mu), \mathbf{s}_\mu, \mathbf{r})\varphi_\mu(B_{1s_{1/2}}, \rho(\mathbf{p}_\mu), \mathbf{s}_\mu, \mathbf{r}) \Rightarrow \mathrm{F} = 4\pi\langle r\rangle^2$$

With the choice of F, formula (24) gives not a precise correction procedure for the various BOMES, but an upper limit for the change of the shape of the spectra. In Fig. 4 we have drawn this maximum correction for sulphur ^{32}S assuming $(V-A)$ interaction. Formula (24) in context with the expression (25) should not be taken too seriously in the low energy region $E_e \lesssim 30[m_e]$, because equation (25) is not valid in this form: the effect of screening cannot be incorporated in a simple way in this energy region. For further reading on this subject the reader is referred to Ref. [16].

V. Discussion

Our calculations of the BOMES neglecting electron bremsstrahlung are in agreement with similar calculations performed earlier by several authors ([6], [13]). In addition we have calculated the BOMES in various coupling schemes for several elements, which will probably be chosen for further muon electron conversion experiments ([9], [10]) and also for experiments on bound muon decay ([8]). In an estimate we have shown that the electron bremsstrahlung effect on the BOMES shape may play an important role.

Our calculations are compared with three experimental results: In the first experiment (Ref. [17]) the ratio

$$\Lambda^{\mathrm{Fe}} \equiv \Gamma(\mu^- + {}^{56}\mathrm{Fe} \to e^- + {}^{56}\mathrm{Fe} + \bar{\nu}_e + \nu_\mu)/\Gamma(\mu^- \to e^- + \bar{\nu}_e + \nu_\mu)$$

has been determined; one has found the value $\Lambda_{\mathrm{exp}}^{\mathrm{Fe}} = 0.972 \pm 0.042$ in agreement with our theoretical value $\Lambda_{\mathrm{th}}^{\mathrm{Fe}} = 0.984$. In the second experiment ratios of the form

$$\Lambda^{Z,Z'} \equiv \Gamma(\mu^- + Z \to e^- + Z + \bar{\nu}_e + \nu_\mu)/\Gamma(\mu^- + Z' \to e^- + Z' + \bar{\nu}_e + \nu_\mu)$$

have been measured. The only ratio we can compare is $\Lambda^{\mathrm{Fe,Zn}}$ where one has found experimentally $\Lambda_{\mathrm{exp}}^{\mathrm{Fe,Zn}} = 0.94 \pm .05$ [18]. Our calculations predict a ratio $\Lambda_{\mathrm{th}}^{\mathrm{Fe,Zn}} = 0.990$.

The only experiment on the BOMES was made by the Bern group at SIN in connection with their muon electron conversion experiment [2]. The measured high energy tail of the BOMES for sulphur ^{32}S agrees with the two theoretical bremsstrahlung non-corrected curves of BOMES_{V-A} and BOMES_T. The bremsstrahlung correction leads to a slightly better agreement. In this experiment it was not possible to resolve the tensorial spectrum and the usual $V-A$ spectrum, because the experimental uncertainty was 35% [19], but the pure scalar and pseudo scalar spectra are, as was to be expected, clearly excluded.

Acknowledgements

We are very grateful to J. Schacher, B. Hahn and K. P. Lohs for many helpful discussions on the subject.

Appendix A: Notation

As units we have the system of natural units, i.e. $\hbar = c = m_e = 1$, where m_e is the electron mass.

If not otherwise stated, four-vectors are written as normal letters, whereas three-vectors are written bold face. The metric tensor $g_{\mu\nu}$ (Greek indices range between 0 and 3) and the Dirac matrices γ_μ, γ_5 are exactly the same as of Björken–Drell [12]. The normalization of the Dirac spinors corresponds also to that of Ref. [12]. The interaction operators and the corresponding coupling constants are defined in the following table:

Interaction	S	P	$V-A$	T
Interaction operator	1	γ_5	$\gamma_\mu(1-\gamma_5)$	$\sigma_{\mu\nu} = i[\gamma_\mu, \gamma_\nu]/2$
Coupling constant of this paper	g_S	g_P	g_{VA}	g_T
Connections of our coupling constants to that of Ref. [11]	$g_S^2 = 2\{\lvert C_S\rvert^2 + \lvert C_S'\rvert^2\}$	$g_P^2 = 2\{\lvert C_P\rvert^2 + \lvert C_P'\rvert^2\}$	$g_{VA}^2 = \frac{1}{2}\{\lvert C_V\rvert^2 + \lvert C_V'\rvert^2 + \lvert C_A\rvert^2 + \lvert C_A'\rvert^2\}$	$g_T^2 = \frac{1}{2}\{\lvert C_T\rvert^2 + \lvert C_T'\rvert^2\}$

Instead of taking the charge retention ordered expression $(\bar{\psi}_e(C_i + C_i'\gamma_5)\Gamma_i\psi_\mu)(\bar{\psi}_{\nu_\mu}\Gamma^i\psi_{\bar{\nu}_e})$ where $\Gamma_i = 1, \gamma_5, \gamma_\mu, \gamma_\mu\gamma_5$ or $\sigma_{\mu\nu}$ we could also take the charge exchange ordered term $(\bar{\psi}_e(\tilde{C}_i + \tilde{C}_i\gamma_5)\Gamma_i\psi_{\bar{\nu}_e})(\bar{\psi}_{\nu_\mu}\Gamma^i\psi_\mu)$. The coefficients $\tilde{C}_i$, $\tilde{C}_i'$ however can be expressed by the coefficients C_i and C_i' (see e.g. Ref. [7]); we choose therefore for our case the technically simpler charge retention ordered Lagrangian of equation (1).

Appendix B: The wave function of the electron and the muon

Electron wave function

The relativistic continuum wave function of the electron with total angular momentum $j_{\kappa_e} = |\kappa_e| - \frac{1}{2}$ in a central symmetric potential is given by Ref. [20]:

$$\tilde{\psi}_{\kappa_e\mu_e}(\mathbf{r}) = \begin{pmatrix} g_{\kappa_e}(r)\chi_{\kappa_e}^{\mu_e}(\hat{\mathbf{r}}) \\ if_{\kappa_e}(r)\chi_{-\kappa_e}^{\mu_e}(\hat{\mathbf{r}}) \end{pmatrix} \quad \text{with} \quad \mathbf{r} = r\hat{\mathbf{r}}$$

$$\text{and} \quad \chi_{\kappa_e}^{\mu_e}(\hat{\mathbf{r}}) = \sum_\tau \sqrt{2j_{\kappa_e}+1}\,(-1)^{l_{\kappa_e}-1/2+\mu_e}\begin{pmatrix} l_{\kappa_e} & \frac{1}{2} & j_{\kappa_e} \\ \mu_e - \tau & \tau & -\mu_e \end{pmatrix} Y_{l\kappa_e,\mu_e-\tau}(\hat{\mathbf{r}})\,|\tfrac{1}{2}\tau\rangle \quad \text{(B1)}$$

Here $l_{\kappa_e} = j_{\kappa_e} + \frac{1}{2}\,\mathrm{sign}\,(\kappa_e)$ and $|\frac{1}{2}\tau\rangle$ is the two-component Pauli spinor. The radial

functions $u_{\kappa_e}(r) = rg_{\kappa_e}(r)$ and $v_{\kappa_e}(r) = rf_{\kappa_e}(r)$ are solutions of the differential equations:

$$\frac{d}{dr}\begin{pmatrix} u_{\kappa_e}(r) \\ v_{\kappa_e}(r) \end{pmatrix} = \begin{pmatrix} -\kappa_e/r & E_e + 1 - V(r) \\ -(E_e - 1 - V(r)) & \kappa_e/r \end{pmatrix}\begin{pmatrix} u_{\kappa_e}(r) \\ v_{\kappa_e}(r) \end{pmatrix} \tag{B2}$$

We have used the following potential $V(r)$:

$$V(r) = \begin{cases} -Z\alpha/r & r > R_N \quad ① \\ -\dfrac{Z\alpha}{2R_N}\left(3 - \dfrac{r^2}{R_N^2}\right) & r < R_N \quad ② \end{cases} \tag{B3}$$

R_N is the radius of the nucleus with charge number Z and α is the fine structure constant. In the case where $V(r)$ is given by equation (B3) ① the solutions $u^C_{\kappa_e}(r)$ and $v^C_{\kappa_e}(r)$ are well known [20]; we give here power series solutions for $u^C_{\kappa_e}(r)$ and $v^C_{\kappa_e}(r)$, because they are useful in the case where $E_e \sim 1[m_e]$. Thus they are suitable for giving start values in order to solve equation (B2) with equation (B3) ① numerically; using the notation $p_e = |\mathbf{p}_e|$ one gets:

$$u^C_{\kappa_e}(r) = u_{\kappa_e}(r, \gamma) = \left(\frac{E_e + 1}{\pi p_e}\right)^{1/2} \frac{2^\gamma e^{\pi\eta/2}\,|\Gamma(\gamma + i\eta)|}{\Gamma(2\gamma + 1)} \times (\gamma \cos\varphi - \eta \sin\varphi) \sum_{n=0}^{\infty} a_n (p_e r)^{n+\gamma} \tag{B4a}$$

$$v^C_{\kappa_e}(r) = v_{\kappa_e}(r, \gamma) = \left(\frac{E_e - 1}{\pi p_e}\right)^{1/2} \frac{2^\gamma e^{\pi\eta/2}\,|\Gamma(\gamma + i\eta)|}{\Gamma(2\gamma + 1)} \times (\gamma \cos\varphi - \eta \sin\varphi) \sum_{n=0}^{\infty} b_n (p_e r)^{n+\gamma} \tag{B4b}$$

The coefficients a_n and b_n are given by the following coupled recursion relation:

$$\begin{pmatrix} a_{n+1} \\ b_{n+1} \end{pmatrix} = \frac{1}{(n+1)(n+1+2\gamma)} \times \begin{pmatrix} -Z\alpha[(E_e - 1)/(E_e + 1)]^{1/2} & (n + 1 + \gamma - \kappa_e) \\ -(n + 1 + \gamma + \kappa_e) & -Z\alpha[(E_e + 1)/(E_e - 1)]^{1/2} \end{pmatrix}\begin{pmatrix} a_n \\ b_n \end{pmatrix} \tag{B4c}$$

$$a_0 = 1, \qquad b_0 = \frac{(E_e + 1)}{E_e} \cdot \frac{\eta(\gamma + \kappa_e)}{(Z\alpha)^2}$$

The functions γ, η and φ are defined as follows:

$$\begin{aligned} \gamma &= [\kappa_e^2 - (Z\alpha)^2]^{1/2} \\ \eta &= Z\alpha/p_e \\ e^{2i\varphi} &= \frac{-\kappa_e - i\eta/E_e}{\gamma + i\eta} \end{aligned} \tag{B4d}$$

For later use we write $u_{\kappa_e}^{\substack{\text{irreg}\\ \text{reg}}}(r) = u_{\kappa_e}(r, \mp\gamma)$, $v_{\kappa_e}^{\substack{\text{irreg}\\ \text{reg}}}(r) = v_{\kappa_e}(r, \mp\gamma)$. In the case where $V(r)$ is given by equation (B3) ② the solutions are ([20]):

$$U_{\kappa_e}(r) = \left(\frac{r}{R_N}\right)^{|\kappa_e|} \times \begin{cases} \sum_{n=0}^{\infty} c_n (r/R_N)^{2n} & \kappa_e < 0 \\ \sum_{n=0}^{\infty} \bar{a}_n (r/R_N)^{2n+1} & \kappa_e > 0 \end{cases} \tag{B5a}$$

$$V_{\kappa_e}(r) = \left(\frac{r}{R_N}\right)^{|\kappa_e|} \times \begin{cases} \sum_{n=0}^{\infty} d_n (r/R_N)^{2n+1} & \kappa_e < 0 \\ \sum_{n=0}^{\infty} \bar{b}_n (r/R_N)^{2n} & \kappa_e > 0 \end{cases} \tag{B5b}$$

The corresponding coefficients are determined by the recursion relations

$$\begin{aligned} \bar{a}_n &= \frac{1}{(2|\kappa_e| + 2n + 1)} \{\bar{b}_n (R_N(E_e + 1) + (\tfrac{3}{2}) Z_\alpha) - (\tfrac{1}{2}) Z\alpha \bar{b}_{n-1}\} \\ \bar{b}_{n+1} &= \frac{1}{2(n+1)} \{-\bar{a}_n (R_N(E_e - 1) + (\tfrac{3}{2}) Z\alpha) + (\tfrac{1}{2}) Z\alpha \bar{a}_{n-1}\}, \\ \bar{b}_0 &= \frac{2|\kappa_e| + 1}{R_N(E_e + 1) + (\tfrac{3}{2}) Z\alpha} \end{aligned} \tag{B5c}$$

The coefficients c_n and d_n are given by $c_n(E_e, Z) = \bar{b}(-E_e, -Z)$ and $d_n(E_e, Z) = \bar{a}_n(-E_e, -Z)$. The general solutions of equations (B2)–(B3) are thus given by

$$\begin{aligned} u_{\kappa_e}(r) &= \begin{cases} N_{\kappa_e} U_{\kappa_e}(r) & r < R_N \\ A_{\kappa_e} u_{\kappa_e}^{\text{reg}}(r) + B_{\kappa_e} u_{\kappa_e}^{\text{irreg}}(r) & r > R_N \end{cases} \\ v_{\kappa_e}(r) &= \begin{cases} N_{\kappa_e} V_{\kappa_e}(r) & r < R_N \\ A_{\kappa_e} v_{\kappa_e}^{\text{reg}}(r) + B_{\kappa_e} v_{\kappa_e}^{\text{irreg}}(r) & r > R_N \end{cases} \end{aligned} \tag{B6}$$

The coefficients N_{κ_e}, A_{κ_e} and B_{κ_e} are determined by the continuity conditions of $u_{\kappa_e}(r)$ and $v_{\kappa_e}(r)$ at $r = R_N$ and the postulated asymptotic behaviour of the general radial functions $u_{\kappa_e}(r)$ and $v_{\kappa_e}(r)$. One gets ([21]):

$$\begin{aligned} A_{\kappa_e} &= c_{\kappa_e} B_{\kappa_e}, \qquad N_{\kappa_e} = \frac{c_{\kappa_e} u_{\kappa_e}^{\text{reg}}(R_N) + u_{\kappa_e}^{\text{irreg}}(R_N)}{U_{\kappa_e}(R_N)} B_{\kappa_e} \\ c_{\kappa_e} &= \frac{U_{\kappa_e}(R_N) v_{\kappa_e}^{\text{irreg}}(R_N) - u_{\kappa_e}^{\text{irreg}}(R_N) V_{\kappa_e}(R_N)}{u_{\kappa_e}^{\text{reg}}(R_N) V_{\kappa_e}(R_N) - U_{\kappa_e}(R_N) v_{\kappa_e}^{\text{reg}}(R_N)}, \\ B_{\kappa_e} &= [1 + c_{\kappa_e}(c_{\kappa_e} + 2\cos(\delta_{\kappa_e}^{\text{reg}} - \delta_{\kappa_e}^{\text{irreg}})]^{-1/2} \\ \delta_{\kappa_e}^{\substack{\text{reg}\\ \text{irreg}}} &= -\arg\Gamma(\pm\gamma + i\eta) + \varphi(\pm\gamma) + \pi(l_{\kappa_e} + 1 \mp \gamma)/2 \end{aligned} \tag{B6a}$$

The nuclear radius R_N of a muonic atom, whose nucleus is described by a

two-parameter Fermi charge distribution $\rho_F^{c,t}(r)$ (equation (23)), is given by Ref. [22]:

$$R_N = \left(\frac{m+3}{m}\overline{r^m}\right)^{1/m}$$
$$\overline{r^m} = \int dr r^{m+2}\rho_F^{c,t}(r) \Big/ \int dr r^2 \rho_F^{c,t}(r) \quad \text{where} \quad m = 2 - 0.014456 \times Z \tag{B7}$$

The general distorted plane wave function $\varphi_e(p_e, \mathbf{s}_e, \mathbf{r})$ can be written as an expansion into total angular momentum eigenfunctions $\tilde{\psi}_{\kappa_e\mu_e}(\mathbf{r})$:

$$\varphi_e(p_e, \mathbf{s}_e, \mathbf{r}) = 4\pi[\pi/|\mathbf{p}_e|]^{1/2} \sum_{\kappa_e\mu_e} e^{i\delta_{\kappa e}}(-i)^{l_{\kappa e}}\sqrt{2j_{\kappa_e}+1}(-1)^{\mu_e - 1/2}$$
$$\times \begin{pmatrix} l_{\kappa_e} & \frac{1}{2} & j_{\kappa_e} \\ \mu_e - s_e & s_e & -\mu_e \end{pmatrix} Y^*_{l_{\kappa e}\mu_e - s_e}(\hat{\mathbf{p}}_e)\tilde{\psi}_{\kappa_e\mu_e}(\mathbf{r}) \tag{B8}$$

In order to test the numerical procedure for calculating the exact BOMES, it is necessary to examine $u_{\kappa_e}(r, \gamma)$ and $v_{\kappa_e}(r, \gamma)$ in the case $Z = 0$. One finds:

$$u_{\kappa_e}(r, \gamma = \kappa_e) = \left[\frac{E_e + 1}{\pi p_e}\right]^{1/2} \times (-1)^{(1+\mathrm{sgn}(\kappa_e))/2}(p_e r) j_{l_\kappa}(p_e r)$$
$$v_{\kappa_e}(r, \gamma = \kappa_e) = -\left[\frac{E_e - 1}{\pi p_e}\right]^{1/2} \times (p_e r) j_{l_{-\kappa}}(p_e r) \tag{B9}$$

where $j_{l_\kappa}(p_e r)$ is a spherical Bessel function [14].

Muon ground state $(1s_{1/2})$-wave function

The ground state wave function of the muon is given by

$$\varphi_\mu(B_{1s_{1/2}}, \rho(\mathbf{p}_\mu), \mathbf{s}_\mu, \mathbf{r}) = \begin{pmatrix} g_1(r)\chi^{s_\mu}_{-1}(\hat{\mathbf{r}}) \\ if_1(r)\chi^{s_\mu}_{+1}(\hat{\mathbf{r}}) \end{pmatrix} \tag{B10}$$

The equations for the real functions $g_1(r)$ and $f_1(r)$ are given by

$$\frac{d}{dr}\begin{pmatrix} g_1(r) \\ f_1(r) \end{pmatrix} = m_\mu^{1/2}\begin{pmatrix} 0 & E_\mu + m_\mu - V(r) \\ -(E_\mu - m_\mu - V(r)) & -2/r \end{pmatrix}\begin{pmatrix} g_1(r) \\ f_1(r) \end{pmatrix} \tag{B11}$$

In all the 'exact' calculations we have put ([23])

$$V(r) = -Z\alpha\left\{\frac{4\pi}{r}\int_0^r \rho_F^{c,t}(r')r'^2\,dr' + 4\pi\int_r^\infty \rho_F^{c,t}(r')r'\,dr'\right.$$
$$\left. + \frac{2\alpha}{3r}\int_0^\infty \rho_F^{c,t}(r')r'\{F_1(|\mathbf{r}' - \mathbf{r}|) - F_1(|\mathbf{r}' + \mathbf{r}|)\}\,dr'\right\}, \tag{B12}$$
$$F_1(x) = \int_1^\infty dy\, e^{-2xy}\frac{\sqrt{y^2-1}}{y^3}\left(1 + \frac{1}{2y^2}\right)$$

The charge distribution $\rho_F^{c,t}(r)$ is given by equation (23). The differential equations (B11) with the potential (B12) are solved numerically. We have often used the nonrelativistic point nucleus 1s muon wave function; therefore we write down

here the explicit formula of this wave function:

$$\varphi_\mu(B_{1s}, \rho(\mathbf{p}_\mu), s_\mu, \mathbf{r})\Big|_{\substack{\text{non}\\ \text{relativistic}}} = 2(Z\alpha m_\mu)^{3/2} e^{-Z\alpha m_\mu r} \chi_{-1}^{s_\mu}(\hat{\mathbf{r}}) \tag{B13}$$

Appendix C: The angular matrix element $\langle \kappa_f \mu_f | Y_{\lambda\mu} | \kappa_i \mu_i \rangle$

$$\begin{aligned}\langle \kappa_f \mu_f | Y_{\lambda\mu} | \kappa_i \mu_i \rangle &= \int \chi_{\kappa_f}^{\mu_f +}(\hat{\mathbf{r}})\, Y_{\lambda\mu}(\hat{\mathbf{r}}) \chi_{\kappa_i}^{\mu_i}(\hat{\mathbf{r}})\, d\Omega(\hat{\mathbf{r}}) \\ &= (-1)^{\mu_f + 1/2} \left[\frac{(2j_{\kappa_f}+1)(2\lambda+1)(2j_{\kappa_i}+1)}{4\pi}\right]^{1/2} \begin{pmatrix} j_{\kappa_f} & \lambda & j_{\kappa_i} \\ -\mu_f & \mu & \mu_i \end{pmatrix} \\ &\quad \times \begin{pmatrix} j_{\kappa_f} & \lambda & j_{\kappa_i} \\ \frac{1}{2} & 0 & -\frac{1}{2} \end{pmatrix} \{1 + (-1)^{l_{\kappa_i} + l_{\kappa_f} + \lambda}\}/2 \end{aligned} \tag{C1}$$

where $j_{\kappa_{i,f}} = |\kappa_{i,f}| - \frac{1}{2}$, $l_{\kappa_{i,f}} = j_{\kappa_{i,f}} + (\frac{1}{2})\,\mathrm{sgn}\,(\kappa_{i,f})$ and $\chi_{\kappa_{i,f}}^{\mu_{i,f}}(\hat{\mathbf{r}})$ is defined in (B1).

REFERENCES

[1] J. Schacher, Comments Nucl. Part. Phys. *8* (1978), 97.
[2] A. Badertscher, K. Borer, B. Czapek, A. Flückiger, H. Hänni, B. Hahn, E. Hugentobler, A. Markees, U. Moser, R. P. Redwine, J. Schacher, H. Scheidiger, P. Schlatter and G. Viertel Phys. Rev. Lett. *39* (1977), 1385..
and
A. Badertscher, K. Borer, B. Czapek, A. Flückiger, H. Hänni, B. Hahn, E. Hugentobler, H. Kaspar, A. Markees, T. Marti, U. Moser, J. Schacher, H. Scheidiger, P. Schlatter, G. Viertel and W. Zeller, Int. Conf. on High Energy Physics and Nuclear Structure, Vancouver, 1979.
[3] C. F. Porter and H. Primakoff, Phys. Rev. *83* (1951), 849.
[4] H. Ueberall, Nuovo Cimento *15* (1960), 1963.
[5] V. Gilinsky and J. Mathews, Phys. Rev. *120* (1960), 1450.
[6] R. W. Huff, Ann. Phys. *16* (1961), 288.
[7] E. D. Commins, *Weak Interactions* (McGraw Hill, New York, 1973).
[8] M. Hasinoff, TRIUMF-Research Proposal *83* (1976).
[9] K. Gotow, private communication.
[10] P. A. Souder, private communication.
[11] R. E. Marshak, Riazzudin and C. P. Ryan, *Theory of Weak Interactions in Particle Physics* (Wiley-Interscience, New York, 1969).
[12] J. D. Björken and S. D. Drell, *Relativistic Quantum Mechanics* (McGraw Hill, New York, 1964).
[13] P. Hänggi, R. D. Viollier, U. Raff and K. Alder, Phys. Lett. *51B* (1974), 119
and
P. Hänggi, Master Thesis, University of Basel, unpublished.
[14] M. Abramowitz and I. A. Stegun, *Handbook of Mathematical Functions* (NBS, Washington, 1964).
[15] R. Engfer, H. Schneuwly, J. L. Vuilleumier, H. K. Walter and A. Zehnder, Atomic and Nuclear Data Tables *14* (1974), 509.
[16] A. I. Achieser and W. B. Berestezki, *Quantenelektrodynamik* (B. G. Teubner, Leipzig, 1962).
[17] G. Culligan, D. Harting, N. H. Lipman and G. Tibell, Int. Conf. on Elementary Particles, Aix-en-Provence, 1961.
[18] L. B. Egorov, A. E. Ignatenko, A. V. Kuptsov and M. G. Petrashku, Soviet Physics JETP *16* (1963), 811.
[19] H. Scheidiger, Thesis, University of Bern, unpublished.
[20] M. E. Rose, *Relativistic Electron Theory* (J. Wiley and Sons, New York, 1961).
[21] L. Krüger and J. Rothleitner, Z. Phys. *164* (1961), 330.
[22] K. W. Ford and J. G. Willis, Los Alamos Report LAMS-2387 (1960).
[23] L. D. Landau and E. M. Lifschitz, *Relativistische Quantentheorie* (Akademie-Verlag, Berlin, 1971).